Draft version February 1, 2008
Preprint typeset using LATEX style emulateapj v. 08/13/06

THE ROTATION OF SUB-POPULATIONS IN ω CENTAURI*

E. Pancino†
INAF - Bologna Observatory, via Ranzani 1 I-40127 Bologna, Italy

A. Galfo and F.R. Ferraro
Astronomy Department, Bologna University, via Ranzani 1 I-40127 Bologna, Italy

and

M. Bellazzini
INAF - Bologna Observatory, via Ranzani 1 I-40127 Bologna, Italy

Draft version February 1, 2008

ABSTRACT

We present the first result of the Ital-FLAMES survey of red giant branch (RGB) stars in ω Cen. Radial velocities with a precision of $\sim$0.5 km s^{-1} are presented for 650 members of ω Cen observed with FLAMES-Giraffe at the Very Large Telescope. We found that stars belonging to the metal-poor (RGB-MP), metal-intemediate (RGB-MInt) and metal-rich (RGB-a) sub-populations of ω Cen are all compatible with having the same rotational pattern. Our results appear to contradict past findings by Norris et al., who could not detect any rotational signature for metal-rich stars. The slightly higher precision of the present measurements and the much larger sample size, especially for the metal-richer stars, appear as the most likely explanation for this discrepancy. The result presented here weakens the body of evidence in favour of a merger event in the past history of ω Cen.

Subject headings: globular clusters: individual (NGC 5139) – techniques: radial velocities

1. INTRODUCTION

The giant globular cluster (GC) ω Centauri is one of the most studied objects in the Milky Way since the 60s, thanks to its many peculiar properties. As its main anomaly, ω Cen shows a wide abundance spread ($\sim$1 dex) not only in the light elements, but also in the iron-peak elements (Norris & Da Costa 1995; Norris et al. 1996; Suntzeff & Kraft 1996; Smith et al. 2000), pointing towards a chemical evolution history more reminiscent of a dwarf galaxy than a genuine GC. Moreover, its structural, kinematical and dynamical properties appear atypical for a Galactic GC, having properties more similar to Dwarf Elliptical galactic nuclei (Mackey & van den Bergh 2005), and being also an elongated (Geyer et al. 1983; Pancino et al. 2003), rotating system (Merritt et al. 1997) that is not completely relaxed dynamically (Anderson 1997; Ferraro et al. 2006).

Among the most recent, puzzling results we list the detection of complex substructures in all evolutionary sequences, including the red giant branch (RGB, Lee et al. 1999; Pancino et al. 2000; Sollima et al. 2005a), the subgiant branch and turn-off region (SGB, Ferraro et al. 2004; Sollima et al. 2005b) and the main sequence (MS, Bedin et al. 2004; Piotto et al. 2005). These studies have raised new questions that need to be answered, such as the debated age differences among sub-populations (Hilker & Richtler 2000; Hughes & Wallerstein 2000; Sollima et al. 2005b), the possibility that some sub-populations possess an extremely high Helium content (Norris 2004; Piotto et al. 2005) and others.

More related with the present paper, we point out a very interesting study on the correlations between chemical and kinematical properties of ω Cen carried out by Norris et al. (1997), where stars in the cluster were divided in two groups based on their Ca abundance. They showed that metal-poorer stars rotate as the majority of the cluster does, while metal-richer stars do not show any sign of rotation. They also showed that the radial velocity dispersion appears to decrease with metallicity, a very strange behaviour since metal-richer stars tend to be concentrated to the cluster center, which is dynamically hotter.

2. OBSERVATIONS AND DATA TREATMENT

A sample of $\sim$700 red giants was selected from the wide field photometry originally published by Pancino et al. (2000) and Pancino (2003), to derive accurate chemical abundances of stars spanning the whole metallicity range of ω Cen. Special care was taken to include a large fraction of high-metallicity stars, which are the less studied up to now. All program stars are distributed within 15 arcmin from the cluster center. Figure 1 shows the program stars, marked on the B, (B–I) color magnitude diagram (CMD) of Pancino et al. (2000). Following the classification scheme of Pancino et al. (2000) and Pancino et al. (2003), stars are divided in three groups: the metal-poor population (RGB-MP) comprising 75% of the cluster giants, with [Fe/H]$\sim$–1.6; the metal-intermediate population (RGB-MInt) comprising 20% of the cluster giants, with [Fe/H]$\sim$–1.2 and the metal-rich or anomalous stars (RGB-a), 5% of the cluster giants, with [Fe/H]$\simeq$–0.6 (Pancino et al. 2002). Sample sizes are shown in Table 2.

Observations were done with FLAMES (Pasquini et

*Based on data obtained with the Giraffe-FLAMES facility of ESO Very Large Telescope during the Ital-FLAMES GTO programme 71.D-0217(A). Also based on data from the VALD and GEISA databases.

†e-mail: elena.pancino@oabo.inaf.it

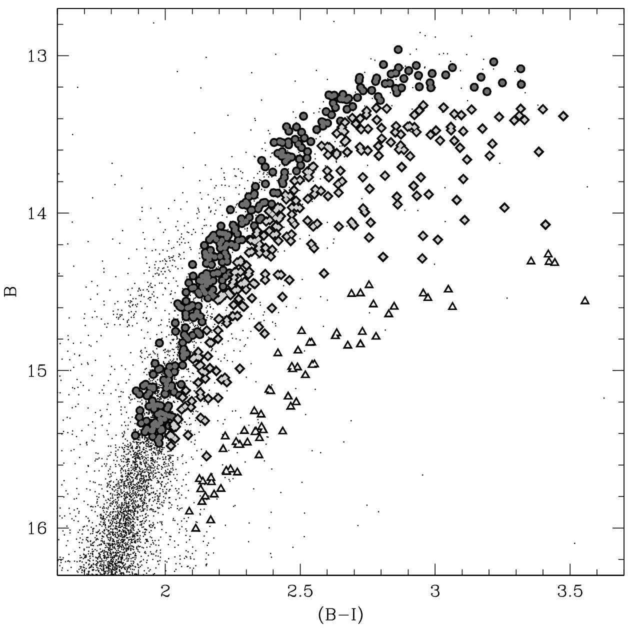

FIG. 1.— Wide Field CMD of ω Cen from Pancino et al. (2000). Stars observed with Giraffe are highlighted: RGB-MP stars with dark grey circles, RGB-MInt with light grey diamonds and RGB-a stars with white triangles.

al. 2002) at the ESO VLT in Paranal, Chile, between the 22nd and 28th of May 2003, within the Guaranteed Observing Time of the Ital-FLAMES Consortium. FLAMES was used in Medusa combined mode, feeding 8 fibers to UVES and 132 fibers to Giraffe. To ensure the maximum homogeneity in data quality and treatment, here we present the first results obtained with Giraffe only, using the high-resolution (R≃22500) grating HR13 (6120–6395Å) and reaching a S/N≃50-100 per pixel, depending on the star magnitude.

Data were reduced with the Giraffe BLDRS (Base-Line Data Reduction Software)[1], that includes cosmic rays removal, bias subtraction, flat field correction, wavelength calibration and pixel resampling. The version of the pipeline we used does not include inter-order background and sky subtraction, but these have no significant effect on radial velocity determinations.

Radial velocities were determined using DAOSPEC[2] (Stetson & Pancino, in preparation), a program that automatically measures equivalent widths of absorption lines in high-resolution spectra. Radial velocities are determined by cross-correlation of the measured line centers and a set of laboratory wavelengths. We used 150 clean and unblended lines of the most common species obtained from the VALD[3] (Vienna Atomic Line Database, Kupka et al. 1999). Observed radial velocities are the average of the velocity obtained for each line after a 3σ clipping, and the associated uncertainty is $\sigma/\sqrt{n}$, where n is the number of lines used. Typical uncertainties are of the order of 0.13 km s^{-1}.

Since radial velocities were not the main goal of the observing programme, simultaneous calibration lamps were not taken during the observations. We used laboratory wavelengths of the telluric lines of the 6300Å O_2 absorption band from the GEISA[4] database (Gestion et Etude des Informations Spectroscopique Atmospheriques, Jaquinet-Husson et al. 2003) to find a common zeropoint to our observed velocities. The typical correction is less than ±1 km s^{-1}, with an uncertainty of $\sim$0.45 km s^{-1}, but we found that for some exposures there were larger offsets, up to 3 km s^{-1}. Finally, we applied the heliocentric correction using the *rvcorrect* task within IRAF[5]. The resulting heliocentric radial velocities have a typical uncertainty of 0.5 km s^{-1} and are reported in Table 1.

TABLE 1
RADIAL VELOCITY MEASUREMENTS

WFI[a]	RA[b]	Dec[b]	B[a]	I[a]	V_r	Pop[c]
—	(deg)	(deg)	(mag)	(mag)	(km s^{-1})	—
100981	201.81686	-47.59584	13.20	10.48	247.377±0.226	1
102141	201.97864	-47.58834	14.51	12.36	237.910±0.382	1
102242	201.84398	-47.58797	14.53	12.35	258.894±0.455	1
103979	201.82367	-47.57775	14.43	12.25	234.816±0.197	1
104113	201.83088	-47.57697	15.35	13.32	239.967±0.781	2

NOTE. — Table 1 is published in its entirety in the electronic edition of the *Astrophysical Journal Letters*. A portion is shown here for guidance regarding its form and content.

[a]WFI star number and B, I magnitudes from Pancino et al. (2000).

[b]Coordinates obtained using the astrometric catalog by van Leeuwen et al. (2000).

[c]Population classification according to Pancino et al. (2000) and Pancino et al. (2003); 1 stands for RGB-MP, 2 for RGB-MInt and 3 for RGB-a (see text for details).

Contaminating field stars were easily eliminated since their average velocity is –4.0±38.5 km s^{-1}, in very good agreement with Galactic model predictions for Disk stars (Robin et al. 2003) and very different from the typical velocity of ω Cen. After removing all stars with $V_r \leq 190$ km s^{-1}, the final sample contains 649 cluster members, with an average V_r=233.4 and σ_r=13.2 km s^{-1}. Star by star comparisons with other catalogues yield a very good agreement. For instance, the average radial velocity difference of the 136 stars in common with Mayor et al. (1997) is ΔV_r=0.4±1.4 km s^{-1}, while for the 53 stars in common with Suntzeff & Kraft (1996) it is ΔV_r=–0.5±1.8 km s^{-1} and for the 382 stars in common with Reijns et al. (2006) it is ΔV_r=–2.4±4.6 km s^{-1}.

3. RESULTS

We used the photometric definition of populations described in Section 2, together with our radial velocity measurements, to construct rotation curves for subpopulations in ω Centauri. To this aim, we first deprojected RA and Dec into X' and Y' coordinates with the following relations (see also van de Ven et al. 2006), suited for extended objects that are not close to the celestial equator:

$$X' = -r_0 \cos\delta \sin(\alpha - \alpha_0)$$
$$Y' = r_0(\sin\delta\cos\delta_0 - \cos\delta\sin\delta_0\cos(\alpha-\alpha_0))$$

[1] http://girbldrs.sourceforge.net
[2] http://cadcwww.hia.nrc.ca/stetson/daospec/; http://www.bo.astro.it/ pancino/projects/daospec.html
[3] http://www.astro.uu.se/∼vald/
[4] http://ara.lmd.polytechnique.fr/htdocs-public/products-/GEISA/HTML-GEISA/
[5] Image Reduction and Analysis Facility. IRAF is distributed by the National Optical Astronomy Observatories, which is operated by the association of Universities for Research in Astronomy, Inc., under contract with the National Science Foundation.

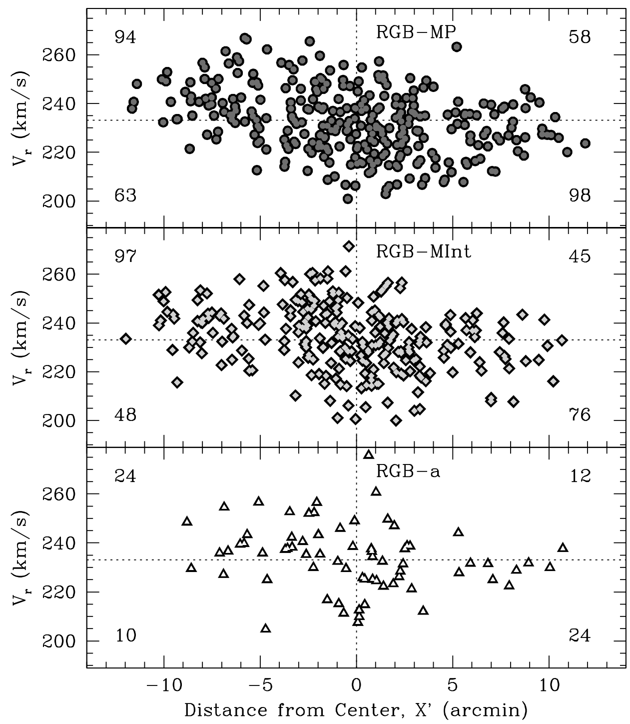

FIG. 2.— Rotation curve for the RGB-MP (top panel), RGB-MInt (middle panel) and RGB-a (bottom panel) samples. The typical rotation pattern of ω Cen can be clearly seen not only for the RGB-MP population, but also for the RGB-MInt and the RGB-a. Each panel is divided in four quadrants by dotted lines passing through the cluster center and the cluster average radial velocity. Each quadrant is labelled with the number of stars it contains.

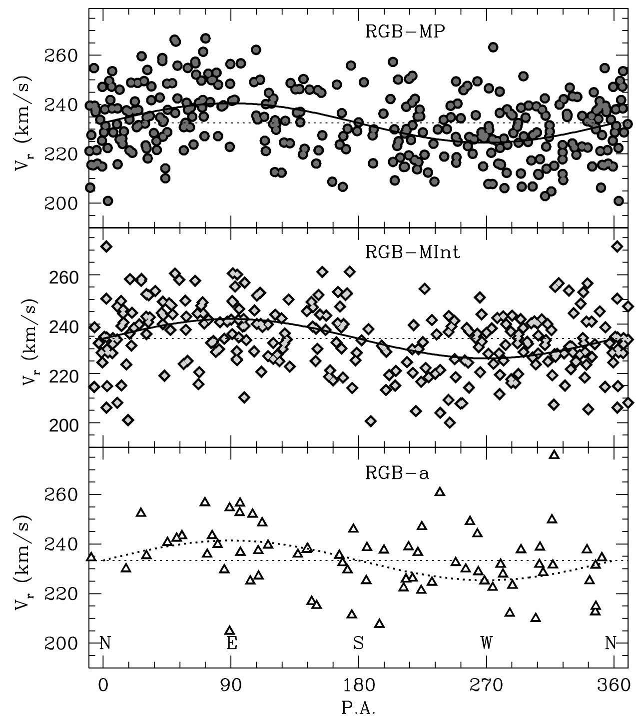

FIG. 3.— Radial velocity measurements are plotted against the position angle (P.A., counted from North towards East) for the RGB-MP (top panel), the RGB-MInt (middle panel) and the RGB-a (bottom panel). Sinusoids with an amplitude of $\sim$8 km s^{-1} (Merritt et al. 1997) are overplotted for reference.

where r_0=10800/π is the scale factor to have X' and Y' in arcminutes.

As a second step, we searched for the orientation of the rotation axis θ that maximizes the amplitude of the rotation signal. We found a relatively broad maximum around $\theta = 0$ and thus, for simplicity, we adopt a rotation axis aligned with the North-South direction, which corresponds to the Y' axis and to the minor isophotal axis (Geyer et al. 1983; Pancino et al. 2003). We therefore plotted radial velocities of each sub-population against X' (Figure 2) and found a clear signature of rotation not only for the RGB-MP, as was expected, but also for the RGB-MInt and the RGB-a. The numbers of stars in the four quadrants of each rotation curve show that the rotational signature is strong even for the most sparse population, i.e., the RGB-a. Assuming that the rotation curves are symmetrical around the minor axis, we estimated the rotation velocity V_{rot} near the maximum (as found by Merritt et al. 1997; van de Ven et al. 2006) as the average of V_r between 6$'$ and 8$'$ from the center (see Table 2). As can be seen, the values of V_{rot} are comparable to each other, within the uncertainties, and are compatible with previous literature estimates.

If the three samples were non-rotating, the histogram of radial velocities on the Eastern half of the cluster would be identical to the Western half (see Figure 2). A Kolmogorov-Smirnov test shows instead that the radial velocity distribution of stars on the Eastern side of the cluster has a very low probability of being extracted from the same parent distribution of the Western side. More quantitatively, the probabilities P_{KS} derived from the cumulative distributions are: 10^{-5} for the RGB-MP, 5×10^{-6} for the RGB-MInt and 5×10^{-3} for the RGB-a.

3.1. *Literature comparison*

A correlation between kinematic properties and chemical abundances in ω Cen has been attempted, to our knowledge, only by Norris et al. (1997) and Sollima et al. (2005b). Norris et al. (1997) correlated the Calcium IR triplet abundances by Norris et al. (1996) with the radial velocity measurements by Mayor et al. (1997), for a global sample of $\sim$400 RGB stars. The sample was split in a metal-poor group with [Ca/H]$\leq$–1.2 and a metal-rich group with [Ca/H]>–1.2. The metal-poor group contains mainly stars that we classify as RGB-MP, with some contamination by RGB-MInt stars, while the metal-rich group contains mainly RGB-MInt and a handful of RGB-a stars, with very little contamination by RGB-MP stars.

The two main results presented by Norris et al. (1997) are *(i)* metal-poor stars rotate, while the metal-rich population does not show any sign of rotation (at a 2 σ level of confidence) and *(ii)* the radial velocity dispersion decreases as metallicity increases, i.e. the metal-rich population is kinematically cooler than the metal-poor one, even if it is concentrated in the central, hotter regions of the cluster[6]. A correlation between radial velocity dispersion and metallicity was also reported by Sollima et

[6] This was referred to as the radial velocity dipersion paradox in ω Cen, and a possible explanation, involving the presence of a face-on metal-rich disk, was presented by van den Bosch et al. (1999).

TABLE 2
Sample sizes, radial velocity and rotation velocity.

Population	n	V_r	σ_r	A_{rot}	V_{rot} ($6'$–$8'$)	n ($6'$–$8'$)
—	—	(km/s)	(km/s)	(km/s)	(km/s)	—
Whole	649	233.4	13.2	∼6	6.8±1.0	87
RGB-MP	313	232.5	13.3	∼7	8.1±1.5	46
RGB-MInt	266	234.2	13.1	∼6	5.3±1.7	33
RGB-a	70	234.0	13.4	∼4	6.0±3.0	8

al. (2005b), who found a similar trend as in Norris et al. (1997), except that the dispersion increases again for the most metal rich stars in their sample.

Velocity dispersions may be quite sensitive to outliers and to the radial distribution of the chosen samples, and a detailed analysis would greatly benefit from the metallicity estimates of individual stars that are not yet available. Here we simply note that there appears to be no difference in the global velocity dispersions of the three subsamples (Table 2). However, the present photometric classification is probably too coarse to reveal subtle effects such as the ones presented by Norris et al. (1997) and Sollima et al. (2005b), hence we postpone any conclusion on radial velocity dispersions to a future paper. On the other hand, strong coordinate motions like the rotation patterns shown in Figure 2 are clearly very robust to the effect of a few outliers and can be profitably studied with the available information. Even in the absence of individual metallicity estimates, Figure 2 leaves very little room for a non-rotating sub-population within ω Cen. To facilitate a comparison with Figure 3 by Norris et al. (1997), Figure 3 shows the run of V_r with the position angle (P.A.) for the three populations of ω Cen. As before, all populations show the well known rotation along the East-West direction (Norris et al. 1997; Merritt et al. 1997). Even the RGB-a, despite the smaller sample, is still compatible with the same rotational pattern. The amplitude A_{rot} of the rotation signal in Figure 3, obtained with a χ^2 minimization, is reported in Table 2. However, A_{rot} can only be considered as an indicative value since it contains contributions from stars at very different radii, and the systemic rotation is highly radius dependent.

We considered two possible reasons why the rotational signature[7] was not found before: sample size and measurement precision. The size of the entire sample is not so different: Norris et al. (1997) had ∼400 stars, we have ∼650. However our sample contains more metal-rich stars: we have 313 stars in the RGB-MP, and 336 stars in the RGB-MInt and RGB-a together, while Norris et al. (1997) had ∼300 metal-poor stars and less than 100 metal-rich stars. Also, the precision of the radial velocity measurements could play a role, although we have an uncertainty of ∼0.5 km s^{-1} and Mayor et al. (1997) have an uncertainty which is only slightly higher and still below 1 km s^{-1}. However, as Norris et al. (1997) made clear, the absence of rotation for the metal-rich group was confirmed only at the 2 σ level, therefore the combination of a slightly higher precision and a much larger sample size are probably enough to explain why we were able to reveal such a signature with our dataset.

4. CONCLUSIONS

We presented the first results from the Ital-FLAMES survey of the RGB of ω Cen. Radial velocities with uncertainties of 0.5 km s^{-1} are derived for 650 radial velocity members of ω Cen, and are in very good agreement with previous literature measurements. The main result obtained is that all the three sub-populations of ω Cen show the same rotation pattern. These findings appear in contradiction with the results presented by Norris et al. (1997). We show that a combination of higher precision in the V_r measurements and of a larger sample size, especially for metal-rich stars (RGB-MInt and RGB-a), is the most likely cause for the discrepancy.

The results by Norris et al. (1997) were the main piece of evidence in support of a merger event in the past evolution of ω Cen. The evidence presented here suggests that there is no rotational anomaly in ω Centauri. The only other remaining evidence, apart from the radial velocity dispersion paradox mentioned above, that still points towards a complicated dynamical history is the structural difference among populations found by Pancino et al. (2003) and the somewhat debated differential proper motion for the RGB-a found by Ferraro et al. (2002), questioned by Platais et al. (2003) but supported by Hughes et al. (2004). Clearly, a deeper investigation into these aspects is now needed to finally settle the issue.

We thank P. B. Stetson, A. Sollima and C. Cacciari. We also thank J. E. Norris, the referee of this paper, for his constructive comments. The financial support from the PRIN-INAF 2005, PRIN-INAF2006 and ASI-INAF I/023/05/0 grants is acknowledged.

Some support to this hypothesis comes from the possible presence of a small disc-like structure in the center of ω Cen pointed out by van de Ven et al. (2006).

[7] As stated before, the data presented in this paper do not allow to reach a firm conclusion on the velocity dispersion, so we will only consider the rotation patterns in the following discussion.

REFERENCES

Anderson, J., 1997, Ph.D. Thesis, Univ. California, Berkeley
Bedin, L. R., Piotto, G., Anderson, J., Cassisi, S., King, I. R., Momany, Y., & Carraro, G. 2004, ApJ, 605, L125
Ferraro, F. R., Bellazzini, M., & Pancino, E. 2002, ApJ, 573, L95
Ferraro, F. R., Sollima, A., Pancino, E., Bellazzini, M., Straniero, O., Origlia, L., & Cool, A. M. 2004, ApJ, 603, L81
Ferraro, F. R., Sollima, A., Rood, R. T., Origlia, L., Pancino, E., & Bellazzini, M. 2006, ApJ, 638, 433
Geyer, E. H., Nelles, B., & Hopp, U. 1983, A&A, 125, 359
Hilker, M., & Richtler, T. 2000, A&A, 362, 895
Hughes, J., & Wallerstein, G. 2000, AJ, 119, 1225
Hughes, J., Wallerstein, G., van Leeuwen, F., & Hilker, M. 2004, AJ, 127, 980
Jaquinet-Husson, N., Scott, N. A., Chedin, A., & Chursin, A. A. 2003, Atmospheric and Oceanic Optics. 3, 256
Kupka, F., Piskunov, N., Ryabchikova, T. A., Stempels, H. C., & Weiss, W. W. 1999, A&AS, 138, 119
Lee, Y.-W., Joo, J.-M., Sohn, Y.-J., Rey, S.-C., Lee, H.-C., & Walker, A. R. 1999, Nature, 402, 55
Lupton, R. 1993, Princeton, N.J.: Princeton University Press, —c1993,
Mackey, A. D., & van den Bergh, S. 2005, MNRAS, 360, 631
Mayor, M., et al. 1997, AJ, 114, 1087
Merritt, D., Meylan, G., & Mayor, M. 1997, AJ, 114, 1074
Meylan, G., Mayor, M., Duquennoy, A., & Dubath, P. 1995, A&A, 303, 761
Norris, J. E., & Da Costa, G. S. 1995, ApJ, 447, 680

Norris, J. E., Freeman, K. C., & Mighell, K. J. 1996, ApJ, 462, 241
Norris, J. E., Freeman, K. C., Mayor, M., & Seitzer, P. 1997, ApJ, 487, L187
Norris, J. E. 2004, ApJ, 612, L25
Pancino, E., Ferraro, F. R., Bellazzini, M., Piotto, G., & Zoccali, M. 2000, ApJ, 534, L83
Pancino, E., Pasquini, L., Hill, V., Ferraro, F. R., & Bellazzini, M. 2002, ApJ, 568, L101
Pancino, E., Seleznev, A., Ferraro, F. R., Bellazzini, M., & Piotto, G. 2003, MNRAS, 345, 683
Pancino, E. 2003, Ph.D. Thesis, Bologna University
Pasquini, L. et al. 2002, The Messenger 110, 1
Piotto, G., et al. 2005, ApJ, 621, 777
Platais, I., Wyse, R. F. G., Hebb, L., Lee, Y.-W., & Rey, S.-C. 2003, ApJ, 591, L127
Reijns, R. A., Seitzer, P., Arnold, R., Freeman, K. C., Ingerson, T., van den Bosch, R. C. E., van de Ven, G., & de Zeeuw, P. T. 2006, A&A, 445, 503
Robin, A. C., Reylé, C., Derrière, S., & Picaud, S. 2003, A&A, 409, 523
Smith, V. V., Suntzeff, N. B., Cunha, K., Gallino, R., Busso, M., Lambert, D. L., & Straniero, O. 2000, AJ, 119, 1239
Sollima, A., Ferraro, F. R., Pancino, E., & Bellazzini, M. 2005a, MNRAS, 357, 265
Sollima, A., Pancino, E., Ferraro, F. R., Bellazzini, M., Straniero, O., & Pasquini, L. 2005b, ApJ, 634, 332
Suntzeff, N. B., & Kraft, R. P. 1996, AJ, 111, 1913
van de Ven, G., van den Bosch, R. C. E., Verolme, E. K., & de Zeeuw, P. T. 2006, A&A, 445, 513
van den Bosch, F. C., Lewis, G. F., Lake, G., & Stadel, J. 1999, ApJ, 515, 50
van Leeuwen, F., Le Poole, R. S., Reijns, R. A., Freeman, K. C., & de Zeeuw, P. T. 2000, A&A, 360, 472